Proceedings World Geothermal Congress 2026
Calgary, Canada, June 8 – 11, 2026

Simulation Framework for Analyzing Fluid–Drill String Interactions in Geothermal Well Drilling Under Novel Conditions

D. Lastiwka[1]*, A. Leakos[1], P. Fisico[1] and T. Miguens[1]
Eavor Technologies[1]*
Derek.lastiwka@eavor.com

Keywords: simulation, fluid-structure interaction, digital-twin, drilling

ABSTRACT

Validation of steady state low-fidelity numerical simulation tools for deep geothermal drilling is presented. The framework couples several numerical modules: a one-dimensional compressible fluid-flow finite volume model for mud/fluid behavior, a two-dimensional axisymmetric thermal finite element model to capture drill-string temperature, and a six degree of freedom beam finite element model to resolve the drill string mechanical response. Thermal interaction between fluid, drill string, and subsurface domains is treated through two-way coupling, while fluid-structure interaction is captured via one-way methodology. These simplified models enable real-time or faster-than-real-time execution, supporting a digital-twin capability that continuously predicts thermal and mechanical states during drilling. Results show that the low-fidelity, steady state model captures physics reasonably well when compared to higher fidelity models. The results shown here prove that this framework can be a practical tool for planning and risk assessment in geothermal projects operating beyond the limits of conventional tools.

1 INTRODUCTION

Geothermal energy offers a scalable pathway to firm, low-carbon electricity, but lowering the levelized costs requires good drilling performance (IEA, 2024). To access greater geothermal potential energy requires wells that extend into deeper formations and operate at temperatures beyond the envelope of conventional oil and gas practice (IEA, 2024). Simulation of drilling in these deep geothermal environments introduces requirements for coupled thermal, fluid, and mechanical phenomena—along with unconventional fluids and materials—that are not well represented in existing drilling analysis and planning tools. As a result, operators face significant uncertainty when designing, executing, and monitoring geothermal wells under extreme conditions.

Drilling simulation tools have long supported well planning and operational decision-making, yet most current platforms rely on simplified models calibrated to traditional regimes. Alternative options would require high-fidelity physics modeling, which results in low computational speed. For next-generation geothermal projects, this trade-off becomes limiting: high-fidelity models are too slow for operational use, while legacy low-fidelity tools lack the physics needed to remain reliable at high temperature and depth. There is therefore a clear need for modeling frameworks that can capture the dominant coupled behaviors of geothermal drilling while remaining fast enough to support real-time decision cycles.

In response to this gap, Eavor Technologies has developed a modular simulation framework specifically designed for geothermal drilling in novel operational regimes. The framework combines multiple numerical modules that represent the core subsystems of the drilling process. A one-dimensional compressible fluid-flow finite-volume model predicts the primary flow variables of the drilling mud. A two-dimensional axisymmetric thermal finite-element model resolves temperature distributions within the drill string. Mechanical response is computed using a six-degree-of-freedom beam finite-element formulation that estimates stresses and strains along the drill string. These components are coupled through a two-way thermal interaction between mud and drill string, and a one-way fluid-structure coupling that transfers fluid and thermal loads into the mechanical domain.

Crucially, the framework is built around low-fidelity modeling strategies that preserve the governing physics most relevant to geothermal drilling while enabling real-time or faster-than-real-time execution. This performance makes the system suitable for digital-twin deployment, where model predictions can be continuously updated and used to monitor evolving thermal and mechanical states during operations. Such capability supports proactive risk assessment, improved operational planning, and more robust drilling strategies in geothermal wells that push beyond established engineering limits.

This paper presents the architecture and coupling approach of the framework and validates the steady state models, showing how low-fidelity, modular simulations can deliver operationally useful predictions in extreme geothermal conditions.

2 1-D FLUID FLOW SOLVER

The fluid flow solver module solves the 1-D Navier-Stokes equations. This solver neglects diffusion and models wall shear stress using a wall friction model (White, 2011). Therefore, the simplified governing equations for mass, momentum and energy are given by (White, 2011):

$$\nabla \cdot (\rho \mathbf{V}) = 0 \tag{1}$$

$$\nabla \cdot [\, \mathbf{V} \, (\, \rho \mathbf{V}) \,] \; = \; -\nabla P \; + \mathbf{F} \tag{2}$$

$$\nabla \cdot [\, \mathbf{V} \, (\, \rho H \,) \,] \; = \; W + \; Q \tag{3}$$

Where ρ is density, $\mathbf{V}$ is velocity, P is pressure, $\mathbf{F}$ is momentum source terms, H is enthalpy, W is work source terms, and Q is heat transfer source terms. Many additional physical effects (e.g. wall friction, wall heat transfer, viscous heating) can be modeled using modules that modify the source terms, so much of the physics are absorbed into the source terms.

For steady state simulations, the SIMPLE algorithm (Patankar, 2018; Greenshields and Weller, 2022) is used to couple the pressure and velocity fields. Interpolation of fluxes and scalars can be performed via the upwind method (Greenshields and Weller, 2022), linear upwind method (Greenshields and Weller, 2022) or central methods (Hoffman, 2001).

2.1 Fluid Flow Solver Validation

This case represents pipe flow in a heated pipe with $L_{pipe} = 5$ m. The pipe inner radius r_{in} is 0.0254 m. The heated pipe wall (shown in Figure 1) is not modeled in this case. Rather, the heated section is modeled using a specified inner wall temperature given by:

$$T = 300\text{K} + 50\frac{\text{K}}{\text{m}}x \tag{4}$$

The Eavor fluid flow solver results are compared to results obtained using chtMultiRegionSimpleFoam in OpenFOAM v2312 (“OpenFOAM,” 2024), referred to as OF2312 in this paper, and Comsol (“Comsol Multiphysiscs,” 2024). The working fluid is water, with convective heat transfer to/from the pipe wall modeled using the Gnielinski correlation (Gnielinski, 1976) for the Nusselt (Nu) number, and wall friction modeled using the Haaland correlation (White, 2011) for the friction factor. A schematic of the simulation geometry is shown in Figure 1. The inlet length L_{inlet} is 3 m in the OpenFOAM model to ensure the flow is fully developed before entering the thermal pipe section. The Eavor fluid flow solver and Comsol both assume the flow is fully developed for every computational element.

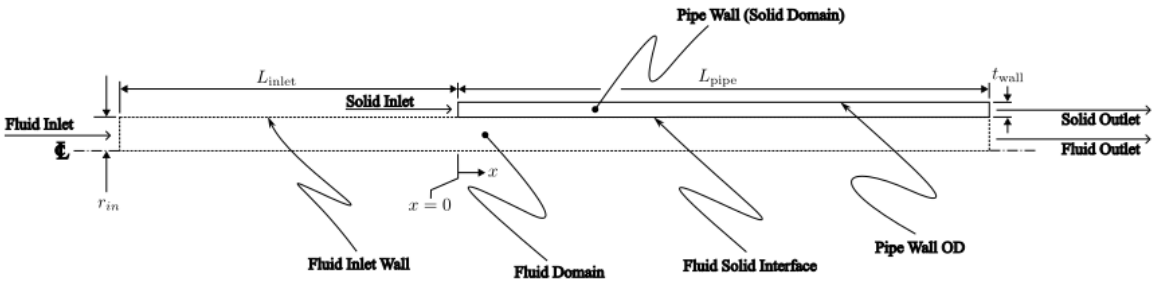


Figure 1: Fluid flow solver validation geometry

2.1.1 Spatial Discretization

Because the Eavor fluid flow solver and the Comsol solver both utilize a 1-D fluid flow methodology a 1-D mesh is used for spatial discretization. The Comsol simulation utilizes 500 line elements to discretize the pipe while the Eavor fluid flow solver utilized 30 line elements.

OpenFOAM is a 3-D finite volume solver and therefore requires a 3-D mesh. To reduce the OpenFOAM computational domain size an axisymmetric analysis was conducted. Due to limitations with OpenFOAM this required creating a wedge domain that is rotated 5 degrees about the x-axis. The domain is composed of 1 cell in the rotation direction. The OpenFOAM mesh consists of 170950 cells for the fluid domain.

2.1.2 Fluid Flow Solver Validation Results

A comparison of the fluid flow validation case results between the three solvers is shown in Figure 2. The results from the Eavor fluid flow solver and Comsol show near perfect agreement. While the OpenFOAM velocity results agree with the other two solvers, the pressure gradient and fluid temperature are over-predicted when compared to the other two solvers. The OpenFOAM pressure gradient may be over predicted because the Haaland friction factor correlation produces a wall shear stress that exactly matches the wall shear stress obtained from the flow profile obtained from the high fidelity OpenFOAM simulation. The reason for the discrepancy in the fluid temperature between the OpenFOAM results and the other two solvers remains unknown currently and requires more investigation. That said it is encouraging that the Eavor fluid flow solver produces near identical results to Comsol, which uses a similar 1-D flow solver methodology.

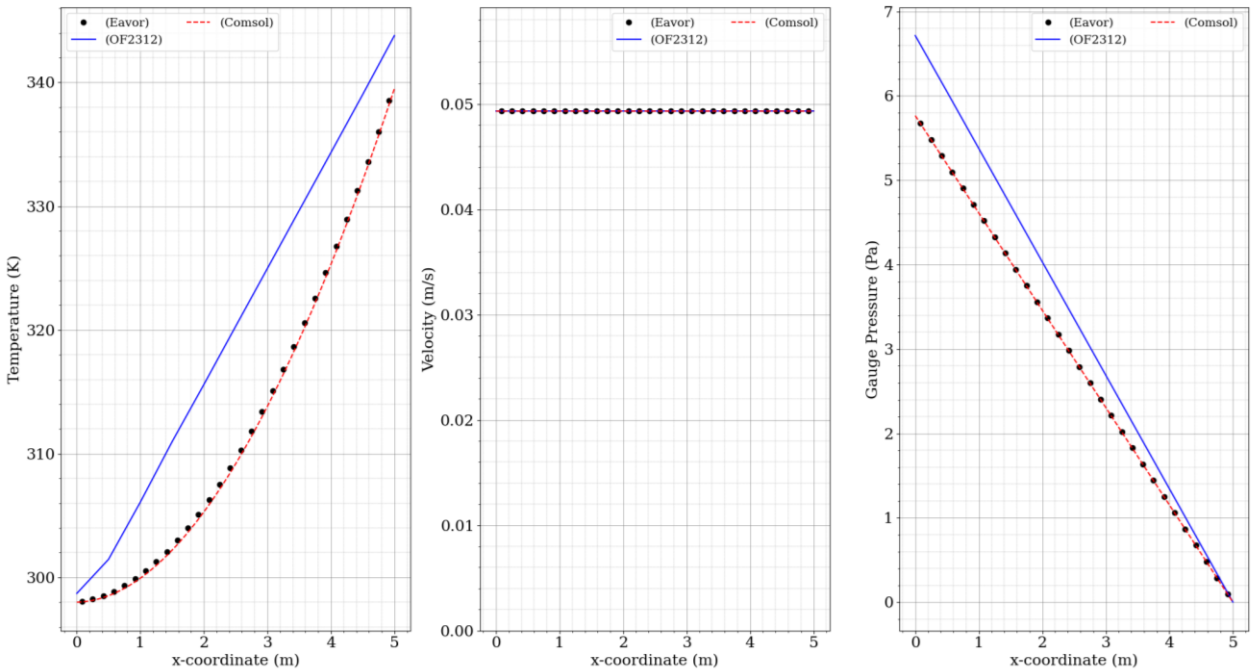


Figure 2: Fluid flow validation case results comparison

3 2-D AXISYMMETRIC HEAT FLOW SOLVER

The thermal field is calculated by solving the 2-D axisymmetric heat equation given by (Hughes, 2000):

$$\nabla \cdot (\boldsymbol{k}\nabla T) + Q = 0 \tag{5}$$

Where $\boldsymbol{k}$ is the thermal conductivity, and T is the temperature. Eqn. 5 is solved using the method of weighted residual with the Bubnov-Galerkin approximation (Hughes, 2000). Non-linear source terms and thermal conductivity can be modeled as well as cross sections with multiple materials.

3.1 Heat Flow Solver Validation

The validation case for the 2-D axisymmetric heat flow solver module represents an insulated drill pipe (IDP) with uninsulated ends. A cross-sectional view of the model (slicing through the axis of rotation) is shown in Figure 3. The steel pipe has an inner radius ($r_{in,\text{pipe}}$) of 0.1 m and an outer radius ($r_{out,\text{pipe}}$) of 0.3 m. The length of the pipe (x_{pipe}) is 5 m. Thermal conductivity of the pipe is 14 W/mK. The insulation inside the pipe starts at $x_{min,\text{ins}} = 0.5$ m and has a length (x_{ins}) of 4 m. The inner ($r_{in,\text{ins}}$) and outer ($r_{out,\text{ins}}$) radii are 0.15 m and 0.16 m respectively. The insulation thermal conductivity is 0.1 W/mK.

The boundary condition on the pipe inner radius is a convection type boundary with a convection coefficient of 5 W/m^{2}K and a farfield temperature of 293 K. The pipe outer wall boundary condition is also a convection type

boundary with a convection coefficient of 25 W/m^{2}K and a farfield temperature of 773 K. The pipe boundary condition at $x = 0$ m and $x = 5$ m are specified flux boundaries with values of 1000 W/m^2 and -1000 W/m^2 respectively. The Eavor heat flow solver results are compared to Calculix.

3.1.1 Spatial Discretization

The Eavor model is discretized with 300 2-D linear quad elements while the Calculix model is discretized with 21,316 3-D linear tetrahedral and hexahedral prism elements.

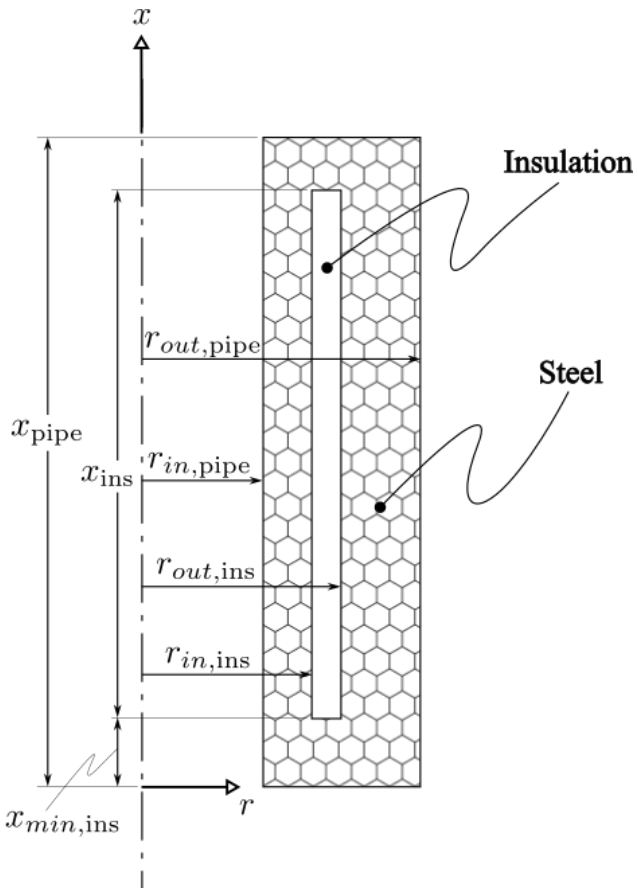


Figure 3: IDP geometry

3.1.2 Heat Flow Solver Validation Results

The results of the Eavor heat flow solver are comparable to the Calculix result with a maximum error (difference) of less than 3% as seen in Figure 4. The error is calculated assuming the Calculix results are the reference data set:

$$\epsilon = \frac{T_{eavor} - T_{calculix}}{T_{calculix}} \tag{6}$$

This result is promising given that the Eavor model discretization has approximately 70 times fewer elements than the Calculix model. With that said, the coarse discretization in the Eavor model is visible in the smoothness of the contours when compared to the Calculix results. This can obviously be improved by refining the Eavor discretization but may not be required when modeling longer drill strings.

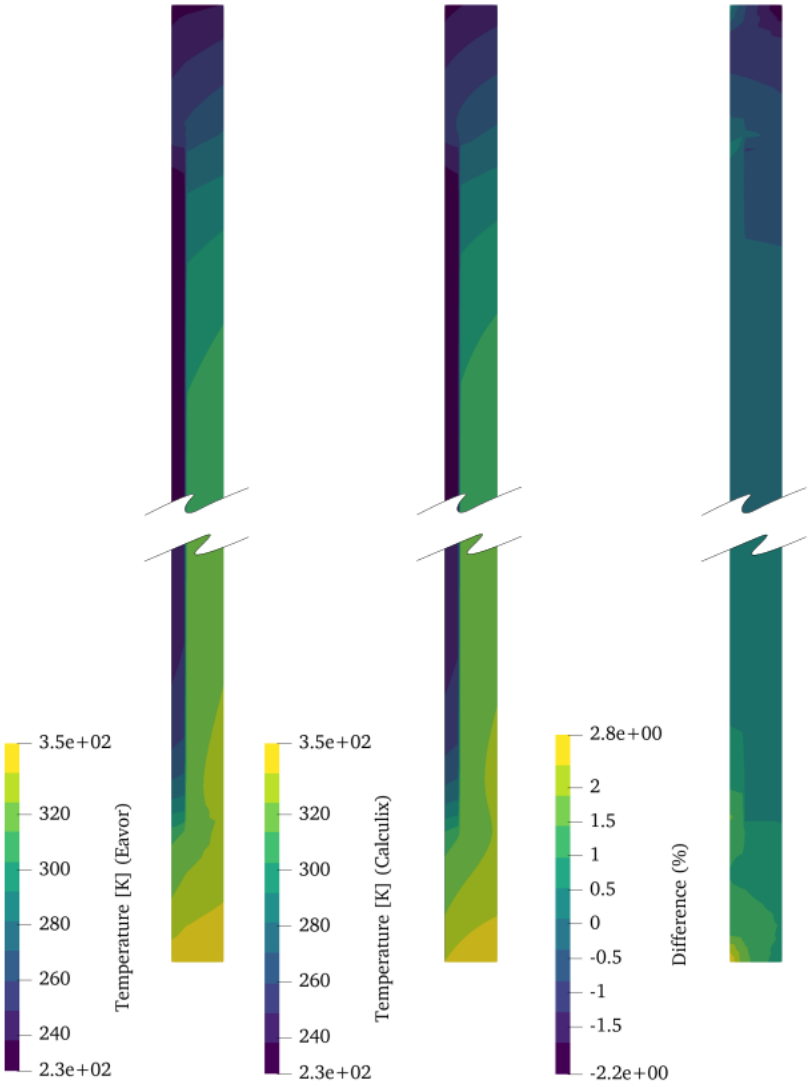


Figure 4: IDP temperature isocontours and difference between the results

4 ELASTOSTATIC BEAM SOLVER

The elastostatic beam solver solves for the balance of forces and moments along the beam. The conservation of forces and moments are given by (Andersen and Nielsen, 2008):

$$\frac{\partial \boldsymbol{F}}{\partial x} + \boldsymbol{q} = 0 \tag{7}$$

$$\frac{\partial \boldsymbol{M}}{\partial x} + \boldsymbol{m} + \boldsymbol{i} \times \boldsymbol{F} = 0 \tag{8}$$

Where the components of $\boldsymbol{F}$ and $\boldsymbol{M}$ are:

$$F = \begin{bmatrix} N \\ Q_y \\ Q_z \end{bmatrix} \tag{9}$$

$$M = \begin{bmatrix} M_x \\ M_y \\ M_z \end{bmatrix} \tag{10}$$

The beam forces and moments are shown in Figure 5. N is the axial force and Q_y and Q_z are shear forces in the y and z directions. The vectors $\boldsymbol{q}$ and $\boldsymbol{m}$ are the distributed forces and moments along the beam. As with the heat

flow equation Eqn. 7 and 8 are solved simultaneously using the method of weighted residuals with the Bubnov-Galerkin approximation (Hughes, 2000).

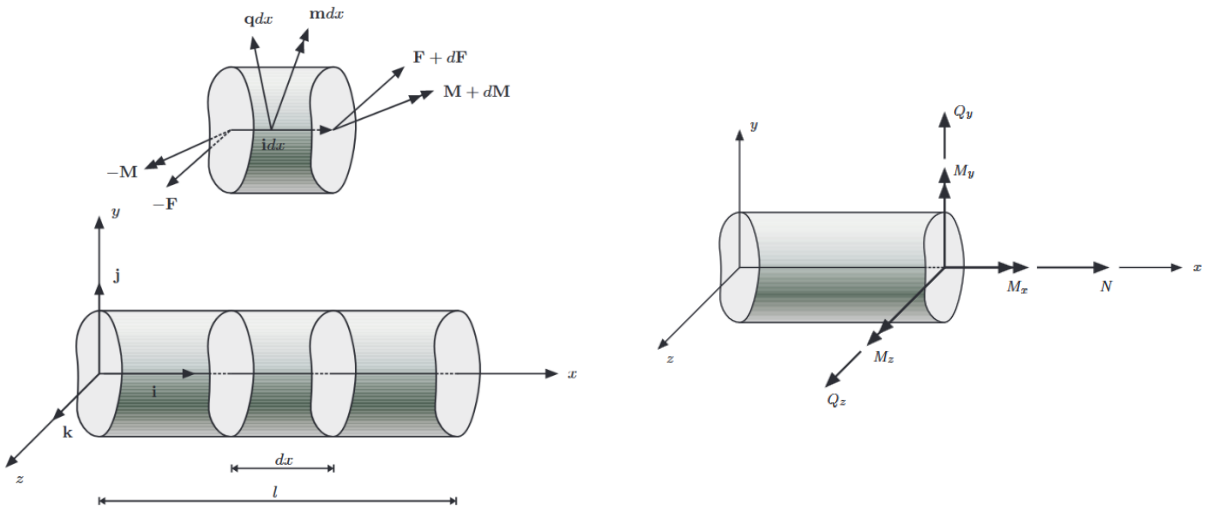


Figure 5: Beam forces and moments - reprinted from Andersen and Nielsen (2008)

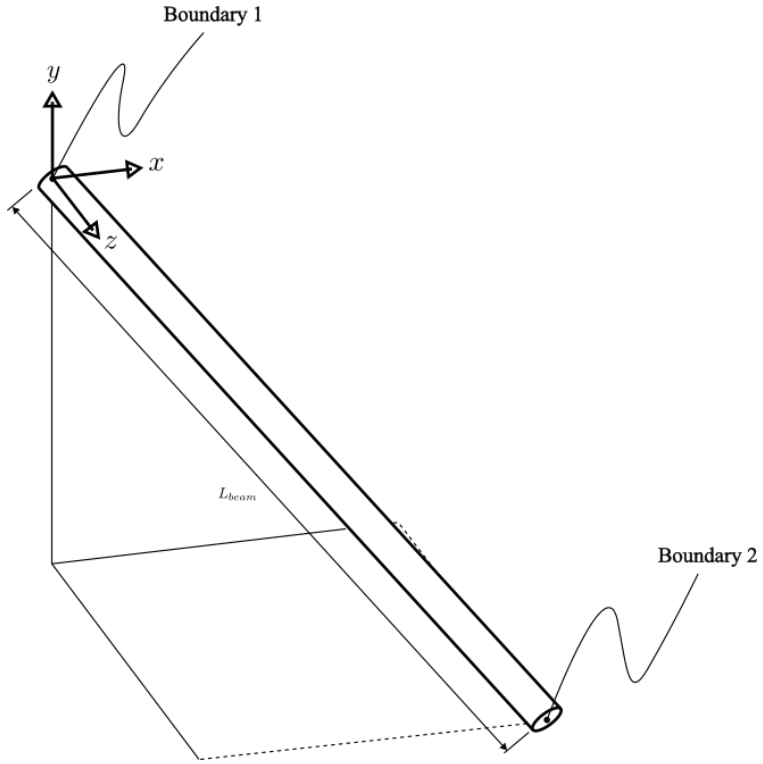


Figure 6: Beam model orientation

4.1 Elastostatic Solver Validation

The beam model validation case consists of a beam originally created with the local x-axis colinear with the global x-axis. The beam was then rotated $\pi/4$ rad about the y-axis followed by $\pi/3$ rad about the x-axis as seen in Figure 6. The beam has a fixed support (all degrees of freedom constrained) at boundary 1 and a load of -5,000 N in the global y-direction applied at boundary 2. A gravitational body force with acceleration due to gravity of -9.81 m/s^2 in the global y-direction was applied as well. The beam is 10 m long with a pipe cross section. The pipe cross section has an inner diameter of 0.0508 m and an outer diameter of 0.0762 m. The results of the Eavor solver were compared against the commercial solver Mecway (“Mecway,” 2024).

4.1.1 Spatial Discretization

Both Mecway and the Eavor solver utilized 100 linear 1-D beam elements for the spatial discretization of the model.

4.1.2 Elastostatic Solver Validation Results

Comparisons of the beam displacements (s_x, s_y, s_z), beam rotations $(\theta_x, \theta_y, \theta_z)$, beam loads and beam moments are shown in Figure 7. The results show essentially perfect agreement between Mecway and the Eavor elastostatic solver.

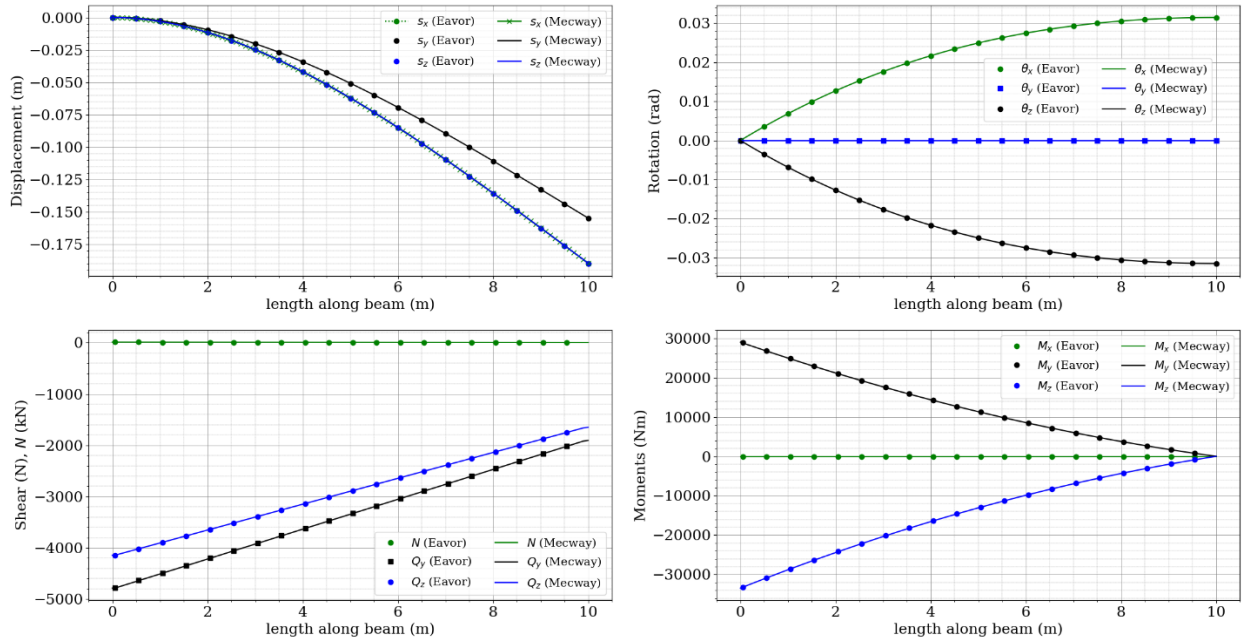


Figure 7: Elastostatic validation case displacements, rotations, loads and moments

5 COUPLED FLUID-THERMAL VALIDATION CASE

This validation case simulates the flow of water (same fluid properties as in section 2.1) down the core of a drill pipe and up the annulus. The wellbore temperature is specified as shown in Figure 9. Heat is transferred between the wellbore and the annular fluid, and between the drill pipe and both the core and annular fluid. A schematic of the geometry is shown in Figure 8. In this case heat transfer within the subsurface domain is not modeled. Simulation parameters are given in Table 1. Results of the Eavor simulation are compared with Comsol.

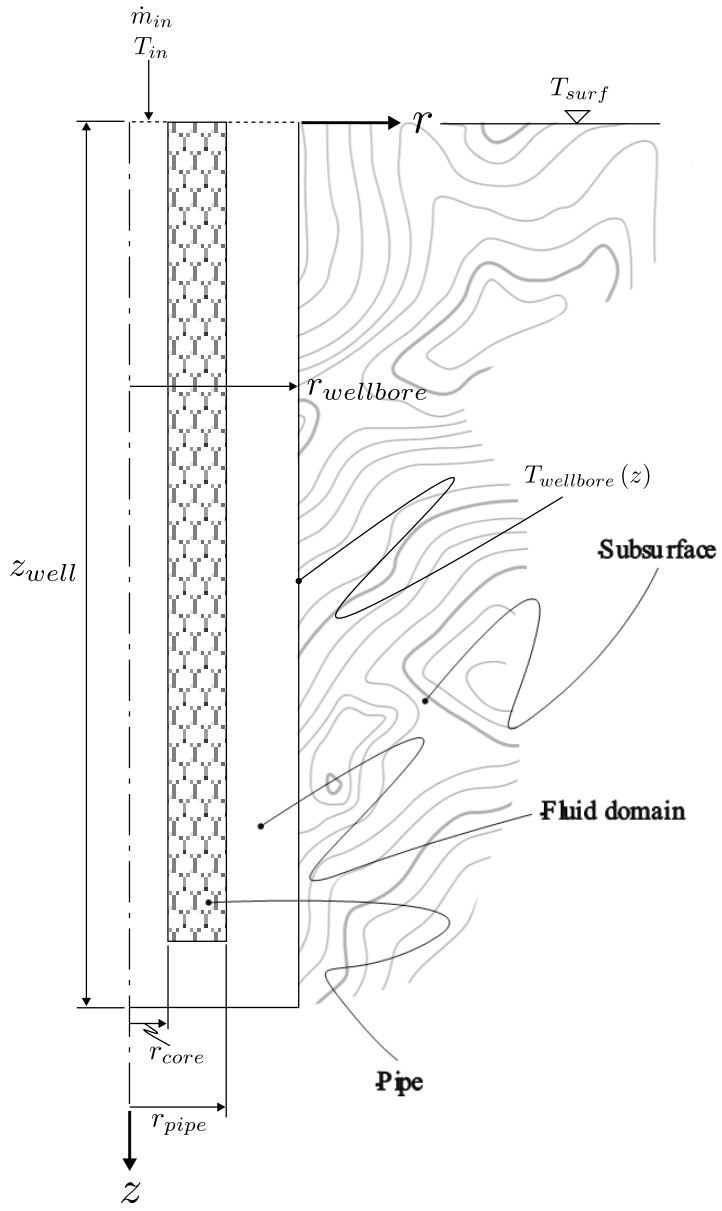


Figure 8: Coupled fluid-thermal validation case geometry

5.1 Spatial Discretization

The Eavor model utilized 50 1-D line elements for each of the fluid core flow and fluid annular flow regions. The Eavor drill string model utilized 500 2-D quad elements for the thermal drill string model. The Comsol model utilized 200 line elements for both fluid domains and the drill string thermal domain.

Table 1: Simulation parameters

Parameter	Value
T_{surf}	293 K
r_{pipe}	0.0762 m
r_{core}	0.0508 m
$r_{wellbore}$	0.107442 m
T_{in}	293 K
$\dot{m}_{in}$	55 kg/s
z_{well}	12 km
Wall roughness	1×10^{-5} m

5.2 Coupled Fluid-Thermal Validation Case Results

A comparison of the results from the Eavor and Comsol coupled fluid-thermal validation case (Figure 9) shows good agreement between the two solvers. The velocity fields are essentially identical between the two solvers. The core pressure drop is slightly higher for the Eavor solver and is likely due to differences in how the wall friction source term is calculated. The Eavor simulation also produces a slightly lower core fluid temperature at the transition between the core and annular regions. This discrepancy in the core fluid temperature requires more investigation. That said, the Eavor solver performs well given the size of the domain and complexity due to physics coupling. Originally the reference case was completed in OpenFOAM 2312. The OpenFOAM case has approximately 450,000 elements. The OpenFOAM simulation case required 15 to 24 hours on a 64 core high performance computing machine to complete and produced similar results to those shown in Figure 9. By comparison, the Eavor simulation required about 2 minutes to complete on a laptop computer. This translates to an approximate 37,000-fold reduction in computing power requirements when using the Eavor low-fidelity modeling methodology compared to the high-fidelity modeling obtained from OpenFOAM.

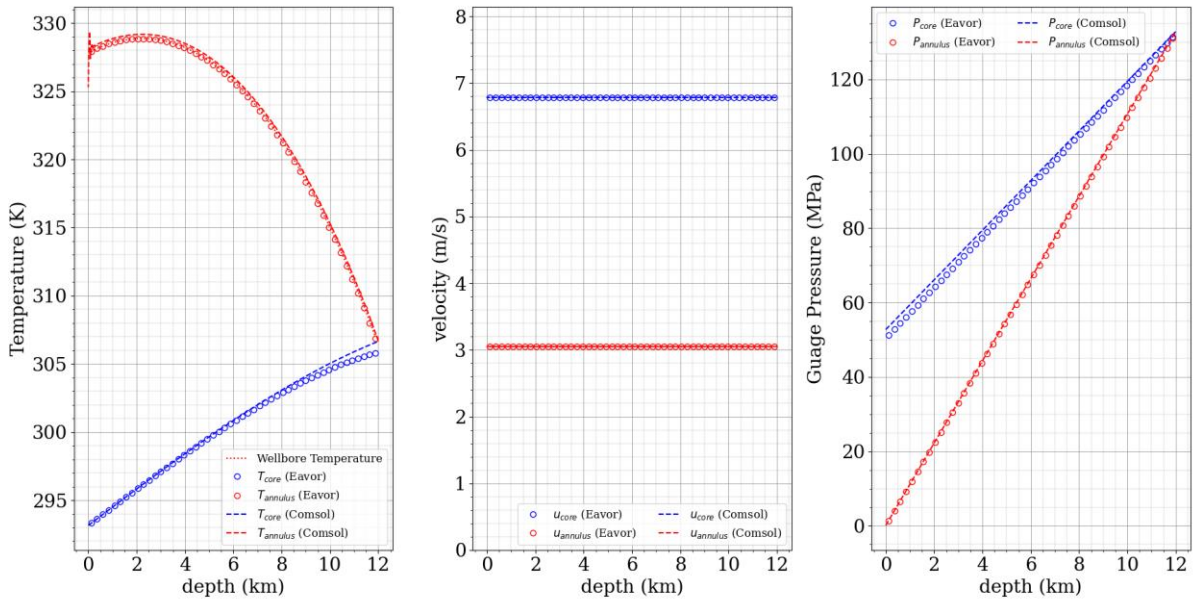


Figure 9: Coupled fluid-thermal validation results

6 CONCLUSIONS

Results of the validation cases show that the Eavor modeling methodology gives comparable results to simulation tools that use similar fidelity modeling or higher, proving that the methodology is sound. In addition, when comparing simulation times to a purely high-fidelity modeling tool (modeling a 2-D axisymmetric domain) the Eavor simulation framework requires roughly 1/37,000 of the computing power needed by a purely high-fidelity tool to complete the same simulation with similar results. Further reduction in computing power requirements from the Eavor simulation framework is expected by utilizing more efficient programming methodologies and potentially different programming languages. While steady state modules were presented here, transient versions have been developed and are in the process of being validated. Additional physics that will be captured include drill string rigid body motion, transient buckling (torsion and lateral modes), multiphase/multicomponent flow, supercritical phases, non-linear drill-string to wellbore contact and friction, and bottom hole assembly physics.

Acknowledgements

The authors acknowledge Amazon Web Services (AWS) for providing cloud computing resources used in this research through the Compute for Climate Fellowship.

REFERENCES

Andersen, L. and Nielsen, S.R.K. (2008) "Elastic Beams in Three Dimensions," *Aalborg University Scientific Publications at the Department of Civil Engineering* [Preprint].

"Comsol Multiphysiscs" (2024). Comsol. Available at: https://www.comsol.com/.

Gnielinski, V. (1976) "New equations for heat and mass transfer in turbulent pipe and channel flow," in. Available at: https://api.semanticscholar.org/CorpusID:136639967.

Greenshields, C.J. and Weller, H.G. (2022) *Notes on computational fluid dynamics: general principles*. Reading, UK: CFD Direct Limited.

Hoffman, J.D. (2001) *Numerical methods for engineers and scientists*. Second edition, revised and expanded. Boca Raton, Florida ; London ; New York: CRC Press.

Hughes, T.J.R. (2000) *The finite element method: linear static and dynamic finite element analysis*. Corr. republication. Mineola (N. Y.): Dover publ.

IEA (2024) *The Future of Geothermal Energy*. France: International Energy Agency. Available at: https://iea.blob.core.windows.net/assets/cbe6ad3a-eb3e-463f-8b2a-5d1fa4ce39bf/TheFutureofGeothermal.pdf.

"Mecway" (2024). Mecway FEA. Available at: https://mecway.com/.

"OpenFOAM" (2024). ESI OpenCFD. Available at: https://develop.openfoam.com/Development/openfoam/-/blob/OpenFOAM-v2312/doc/Build.md?ref_type=tags.

Patankar, S.V. (2018) *Numerical Heat Transfer and Fluid Flow*. Boca Raton, FL: CRC Press.

White, F.M. (2011) *Fluid mechanics*. 7. ed. New York: McGraw-Hill (McGraw-Hill Series in Mechanical Engineering).